Structural Basis of Oncogenic Activation Caused by Point Mutations in the Kinase Domain of the MET Proto-Oncogene: Modeling Studies

Maria Miller,[1] **Krzysztof Ginalski,**[2] **Bogdan Lesyng,**[2,3] **Noboru Nakaigawa,**[4] **Laura Schmidt,**[5] **and Berton Zbar**[4]

[1]*Macromolecular Crystallography Laboratory, National Cancer Institute at Frederick, Frederick, Maryland*
[2]*Department of Biophysics, Institute of Experimental Physics, University of Warsaw, Warsaw, Poland*
[3]*Interdisciplinary Center for Mathematical and Computational Modeling, University of Warsaw, Warsaw, Poland*
[4]*Laboratory of Immunobiology, National Cancer Institute, Frederick at Frederick, Frederick, Maryland*
[5]*Intramural Research Support Program, SAIC Frederick, National Cancer Institute at Frederick, Frederick, Maryland*

ABSTRACT **Missense mutations in the tyrosine kinase domain of the MET proto-oncogene occur in selected cases of papillary renal carcinoma. In biochemical and biological assays, these mutations produced constitutive activation of the MET kinase and led to tumor formation in nude mice. Some mutations caused transformation of NIH 3T3 cells. To elucidate the mechanism of ligand-independent MET kinase activation by point mutations, we constructed several 3D models of the wild-type and mutated MET catalytic core domains. Analysis of these structures showed that some mutations (e.g., V1110I, Y1248H/D/C, M1268T) directly alter contacts between residues from the activation loop in its inhibitory conformation and those from the main body of the catalytic domain; others (e.g., M1149T, L1213V) increase flexibility at the critical points of the tertiary structure and facilitate subdomain movements. Mutation D1246N plays a role in stabilizing the active form of the enzyme. Mutation M1268T affects the S+1 and S+3 substrate-binding pockets. Models implicate that although these changes do not compromise the affinity toward the C-terminal autophosphorylation site of the MET protein, they allow for binding of the substrate for the c-Abl tyrosine kinase. We provide biochemical data supporting this observation. Mutation L1213V affects the conformation of Tyr1212 in the active form of MET. Several somatic mutations are clustered at the surface of the catalytic domain in close vicinity of the probable location of the MET C-terminal docking site for cytoplasmic effectors. Proteins 2001;44:32–43.** © 2001 Wiley-Liss, Inc.*

Key words: MET proto-oncogene; receptor tyrosine kinase; oncogenic mutations; homology modeling; substrate specificity

INTRODUCTION

The MET proto-oncogene/MET encodes a cell membrane receptor tyrosine kinase (RTK) that mediates cell growth, survival, differentiation, and migration in several tissues. Under normal conditions, cell signaling is initiated by binding of the specific ligand, hepatocyte growth factor (HGF), to the extracellular portion of the receptor. Receptor activation then occurs through dimerization, followed by autophosphorylation occurring in *trans* (between two molecules) in the cytoplasmic portion of the protein chain. Autophosphorylation of tyrosine residues within the tyrosine kinase domain—Tyr1248, Tyr1252, and Tyr1253—upregulates the enzymatic activity of the MET receptor. The phosphorylated C-terminus is a docking site for several cytoplasmic effectors responsible for invoking mitogenesis and morphogenesis in epithelial cells (Ref. 1 and references therein). Autophosphorylation of two tyrosines in the C-terminal sequence Y^{1367}VHVNATY^{1374}VNV is necessary for recruiting phosphatidylinositol 3-kinase (PI3K), phospholipase C-γ1 (PLCγ), Src, SHC, and the multiadapter protein GAB1 molecules, whereas the GRB2 protein selectively binds phosphorylated Tyr1374 (pTyr1374). All these signal transducers, with the exception of GAB1, bind to the MET receptor via their respective SH2-homology domains. The tyrosine kinase activity of MET is important for the motility effect,[2] most likely by inducing Ras-dependent activation of cellular gene promoters,[3] and for phosphorylation of GAB1.[4] MET/HGF signaling is essential for normal embryo development, and it was shown that loss-of-function MET mutations cause embryonic lethality.[5,6]

Point mutations located in the catalytic core of MET and other RTKs (RET, c-KIT) have been implicated in human cancers. Several mutations produce ligand-independent activation of the kinase activity of the RTK, leading to uncontrolled cell proliferation and morphological changes.[7–9] Fifteen mutations in 10 codons of MET have been found in patients with hereditary and sporadic forms of papillary renal carcinoma (PRC):[10,11] V1110I(g),

H1112Y(s)/R(g)/L(s), H1124D(s), M1149T(g), V1206L(g), L1213V(s), V1238I(g), D1246N(g)/H(s), Y1248H(s)/D(g)/C(g), M1268T(s) [(s), somatic; (g), germline]. It has been shown that all MET PRC mutations upregulate MET kinase activity,[11–13] but different mutations lead to diverse biological consequences.[12,14] Mutations of codons 1246, 1248, and 1268 cause significant transformation of NIH 3T3 cells,[12,13] whereas the transforming potential of mutations on codons 1112 and 1124 is very small.[11] The M1268T mutant MET displays the highest catalytic activity and the highest transforming potential. Mutations L1213V and Y1248C, which are devoid of transforming ability, are the most effective in increasing cell motility and providing protection from apoptosis.[14] The effect of MET PRC mutations also depends on the level of MET expression as well as the presence of HGF and its activators.[15] Mechanisms of oncogenic signaling via MET PRC mutants are poorly understood.

All protein kinases contain a bilobal conserved catalytic core domain but show significant diversity in the mechanisms of regulation and activation. The relative orientation of the two lobes varies between enzymes and may change significantly during a transition to the active form.[16] Two RTKs with known 3D structures—insulin receptor kinase (IRK)[17,18] and fibroblast growth factor receptor 1 (FGFR1) kinase[19−21]—are inhibited by an intrasteric mechanism and are regulated by transphosphorylation at specific tyrosines within the self-inhibitory peptide, referred to as the activation loop (A-loop). To study the mechanisms by which missense mutations in the MET proto-oncogene produce constitutive activation, we constructed 3D models of the catalytic core domains of the wild-type and mutated MET protein in inhibited and active conformations. We then compared the role played by residues at positions affected by these mutations in maintaining the tertiary structures of inhibited and active forms of the enzyme. Possible mechanisms of malignant transformation caused by PRC mutations are also briefly discussed in this report.

MATERIALS AND METHODS
Homology Modeling
Generating sequence-to-structure alignment

Sequence-to-structure alignment of the target and template proteins is the most significant step in successful homology modeling.[22] Structure-derived sequence alignment of kinase catalytic core domains was generated for protein tyrosine kinases for which crystallographic coordinates were available from the Protein Data Bank (PDB): IRK,[17,18] FGFR1,[19,20] c-Src,[23−25] hematopoietic cell kinase (Hck),[26,27] and lymphocyte kinase (Lck).[28] 3D superposition of the structures was performed separately within the N- and C-terminal lobes by using the Homology module of the Insight II program package.[29] The MET sequence was then aligned with the sequences of IRK, FGFR1, c-Src, Hck, Lck, and c-Abl by using the multiple sequence alignment technique implemented in the CLUSTAL W program.[30] Taking into account the initial structure-derived alignment, the conservation of specific residues, and the placement of secondary structure elements in the
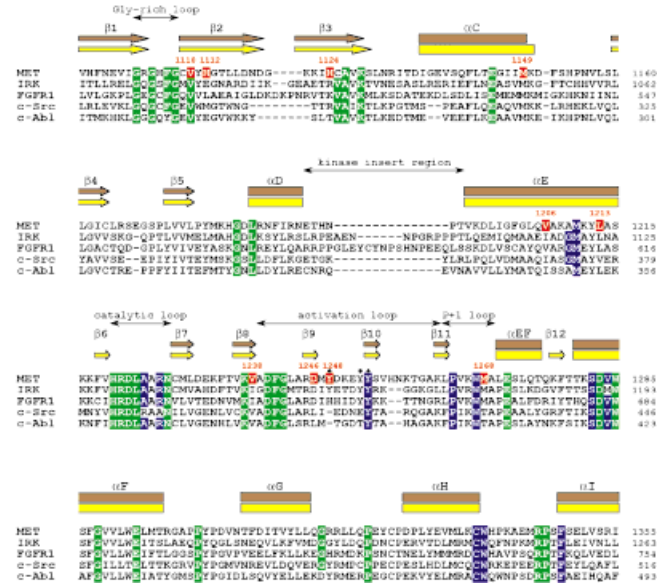

Fig. 1. Sequence alignment of the catalytic core domains of MET, IRK, FGFR1, c-Src, and c-Abl. Residues conserved within the tyrosine kinase subfamily are highlighted in blue, and those for all kinases are in green. The locations of activating mutations in MET are shown in red. Locations of the secondary structure elements in IRK as assessed by DSSP[51] are marked above the sequences: β-strands as arrows and α-helices as rectangles, in yellow and brown for active (PDB code 1IR3) and inhibited (PDB code 1IRK) forms, respectively. Positions of phosphorylated tyrosines are marked by black dots.

kinase catalytic domain, we manually performed some corrections for the alignment of MET and c-Abl sequences.

Building 3D models

Based on the final sequence-to-structure alignment, two models of the MET kinase were built with the Homology module of Insight II by using IRK as a structural template. Modeling of the inhibited form of the MET catalytic core kinase domain was based on the 2.1 Å crystal structure of IRK in its unphosphorylated form (PDB code 1IRK).[17] A model of the active form of the MET catalytic core kinase domain was constructed from coordinates of a ternary complex of the phosphorylated IRK with a peptide substrate and the MgATP analog (PDB code 1IR3).[18] The initial models of wild-type MET kinase were prepared by replacing side chains of IRK with MET side chains according to the alignment shown in Figure 1. Positions of the conserved IRK backbone atoms remained unchanged in the replacement procedure, and the MET side chains followed the IRK side chain positions where possible. The relative insertions and deletions were modeled initially with plausible backbone fragments of the same length extracted from the PDB structures. In the active form of MET kinase, the MgATP analog was substituted with MgATP, and six residues (ATYVNV) from the MET C-terminal self-phosphorylation site were modeled onto the backbone of the IRK peptide-substrate. Subsequently, the positions of several side chains were adjusted manually to remove bad contacts and to maximize the electrostatic and hydrophobic interactions.

Refinement of 3D models

Models were subjected to a series of energy-minimization steps with the Discover module of Insight II[31] until the root-mean-square (RMS) gradient was smaller than 0.001 kcal/(mol · Å). All energy optimizations were performed by using the AMBER force field[32] with a distance-dependent dielectric constant of 4r, using the steepest descent and conjugate gradient methods. New residue types were defined for phosphotyrosine and MgATP (not included in the AMBER library). These molecules were parameterized with respect to precise quantum mechanical calculations using the non-local hybrid density functional B3LYP[33] and 6-31G+ (d,p) basis set implemented in the Gaussian 94 program.[34] The conserved Cα atoms of the protein (and also those of the substrate, in the complex) and the heavy atoms of MgATP were restrained with harmonic forces. To place the A-loop in a conformation with lower energy, we also performed a simulated annealing procedure from 2,000 K to 300 K.

The overall geometrical quality of each model was checked in detail with the WHAT_CHECK program.[35] Regions with unusual geometry were subjected to closer examination, and the conformation of a few side chains was readjusted manually to improve the structural consistency.

Generating and analyzing point mutations

Based on these homology models, the effect of PRC mutations was examined by replacing residues affected by these mutations in the structures of the inhibited and active forms of MET. Detailed rotamer searches for the mutated side chains were performed by using the INSIGHT II package and SCWRL program with the backbone conformation-dependent side chain rotamer library.[36] For some mutations in the inhibited form of MET, no side chain conformations found could be accommodated in the structure without significant changes of the internal packing of the protein and/or a conformational transition.

For the M1268T mutant, its model in complex with a hexapeptide comprising the GPYAQP sequence (derived from a substrate of the c-Abl cytoplasmic tyrosine kinase[37]) was constructed by replacing side chains of relevant amino acids in the model of the ternary complex of the active form of MET kinase. The conformation of the Leu1263 side chain was changed manually to improve the hydrophobic packing disrupted by M1268T substitution (see Results and Discussion). This assembly was then subjected to energy minimization with restrained heavy atoms of MgATP and conserved Cα atoms of the core and the substrate until the RMS gradient was < 0.001 kcal/(mol · Å).

Detailed analysis of the interatomic contacts for residues at the positions affected by the mutations was performed with the LIGIN program.[38] To determine stabilizing and destabilizing interactions, we calculated the contact surface areas independently for legitimate (energetically favorable) and illegitimate (energetically unfavorable) contacts, as assigned by Sobolev et al.,[38] depending on the hydrophobic/hydrophilic properties of the contacting atoms. Complementarity (defined as a result of subtraction of the surface area of illegitimate contacts from the surface area of legitimate ones) was also taken into account. Finally, to evaluate substrate affinities for wild-type and M1268T mutant MET in the modeled structures, we calculated a normalized complementarity (NC), defined as the complementarity divided by the total solvent-accessible surface of the ligand in the uncomplexed state. This approach has been successfully used by others to explain the differences in binding energies of biotin, thiobiotin, and iminobiotin with streptavidin[39] and has also been verified in the CASP2 experiment on ligand-protein structure prediction.[40]

NIH 3T3 Transfections, CrkII Phosphorylation, and Expression

NIH 3T3 cells (CRL 1658) from the American Type Culture Collection were cultured in Dulbecco's Modified Eagle Medium (DMEM)/10% calf serum (Life Technologies, Gaithersburg, MD). The pMB1expression vector containing the wild-type mouse MET cDNA (pMBII) was used for mutation construction using the QuickChange site-directed mutagenesis kit (Stratagene, La Jolla, CA) as previously described.[12] NIH 3T3 cells were transfected with mutant MET constructs by using Lipofectamine (Life Technologies); immunoprecipitation and Western analysis were performed as described[41] under reducing conditions, using anti-Crk II antibody (Transduction Laboratories, Cincinnati, OH) and antiphosphotyrosine antibody (Upstate Biotechnology, Lake Placid, NY). Cells were serum starved to reduce endogenous HGF levels.

RESULTS AND DISCUSSION

The MET kinase domain shares 40% sequence identity (Fig. 1) with the insulin receptor and FGFR1 kinase domains, the only two members of the RTK subfamily for which crystal structures have been determined. Despite high sequence similarity between the catalytic cores of IRK and FGFR1 kinase, crystallographic data revealed significant differences between their inactive conformations. In the unphosphorylated, apo form of IRK, access to ATP and peptide substrate sites is blocked by residues from the A-loop. The three tyrosines from the autophosphorylation site are important for maintaining the inhibitory conformation of the A-loop. In the structure of the inactive form of FGFR1 kinase domain the A-loop follows a different path. The ATP-binding site is open, whereas access to the peptide-substrate-binding site is obscured by residues from the C-terminal part of the A-loop. The paths of the polypeptide chains in these two structures diverge at the residue preceding the protein kinase-conserved DFG motif, which is Gly1149 in IRK and Ala640 in FGRF1 (Fig.1). Because of steric hindrance created by proximity of a branched residue (Val1060 in IRK or Ile545 in FGRF1), Ala640 cannot adopt the same conformation as Gly1149 (IRK).[42] As a consequence, the relative lobe orientation is also different in the two structures. In IRK the two lobes are held apart by steric interactions between residues from the DFG sequence and the glycine-rich loop, whereas in FGRF1, interaction of DFG motif with the αC-helix accounts for less open conformation.[19] In addition, replace-
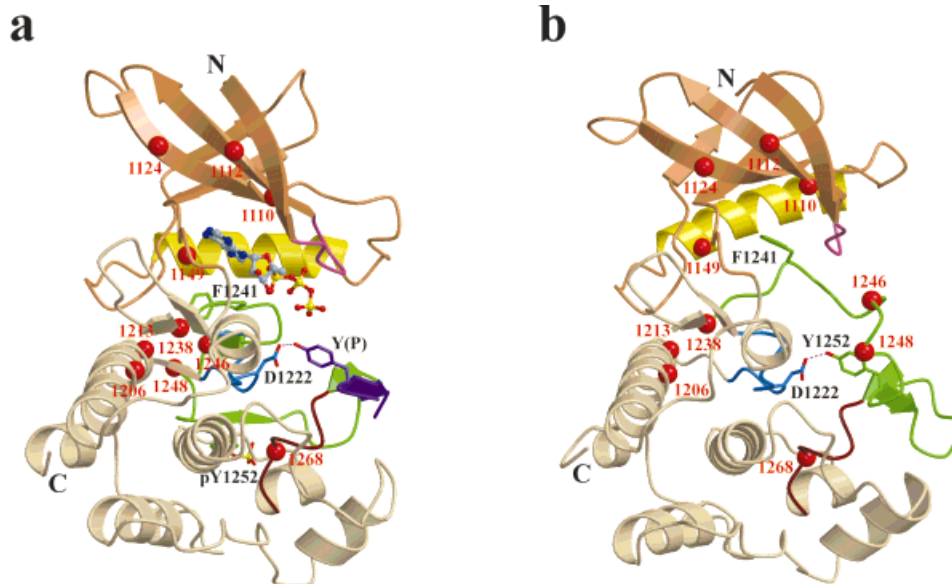
Figure 2.

ment of IRK Tyr1157 by a polar His residue prevents similar interactions with the main body of protein. Thus, differences at specific points in the A-loop sequence of FGFR1 preclude the same conformation as in IRK. On the contrary, MET sequence allows for the inhibitory mechanism with both substrate sites blocked in the same manner as observed in IRK. Although an Ala residue precedes the DFG triplet, the position homologous to Val1060 from IRK is occupied in MET by Leu1158, allowing for similar packing to IRK and the lobe closure. The three specific tyrosine residues in the sequence of MET, homologous to those in the A-loop of IRK, can maintain the same interactions within the active site cleft. The two-residue insertion in the A-loop sequence of MET is located in the region where IRK A-loop is exposed to solvent and is probably disordered. The triphosphorylated A-loop in the active form of IRK structure would be also a better approximation for MET. We therefore based our 3D models of the fully inhibited and active forms of the MET catalytic core
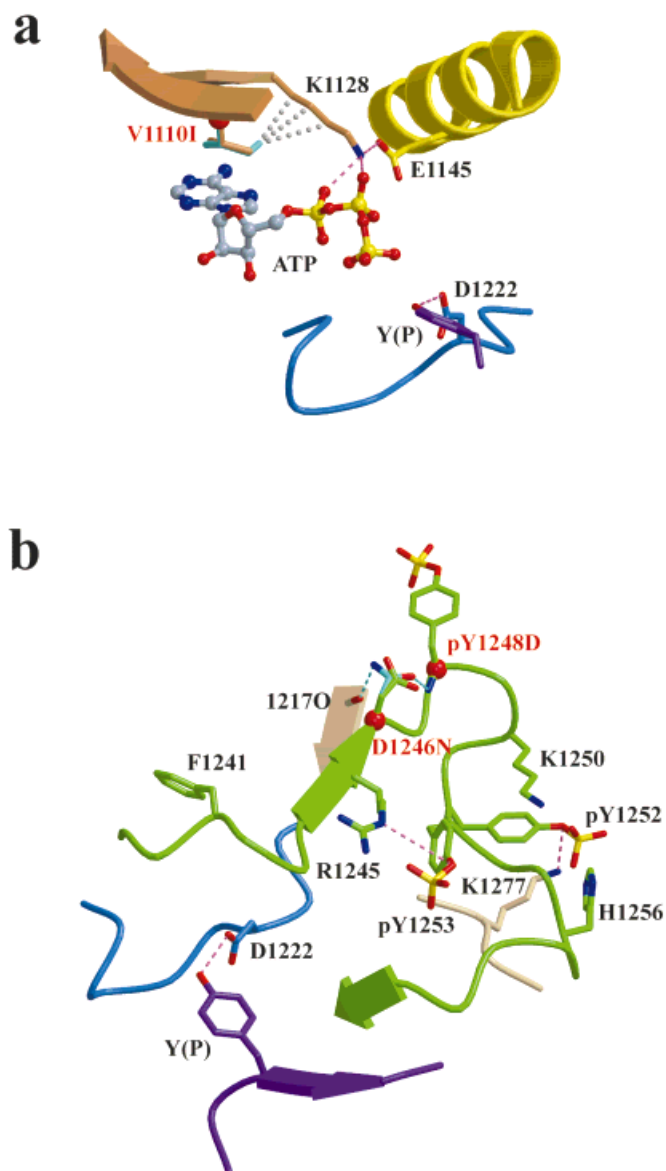

Fig. 2. Ribbon diagrams of 3D models of the kinase domain of MET in its (**a**) active form complexed with MgATP and peptide substrate and (**b**) autoinhibited form. N-terminal and C-terminal lobes are in dark and light beige, respectively; the glycine-rich (nucleotide-binding) loop is in pink, helix C in yellow, catalytic loop in light blue, A-loop in green, P+1 loop in brown, and MET substrate in violet. The termini are denoted by N and C. Selected side chains are represented as sticks, and ATP as balls and sticks. The positions of MET PRC mutations are marked as red spheres. The interaction between the key catalytic residue Asp1222 and tyrosine to be phosphorylated is shown as a pink dashed line.

Fig. 3. Features of the active-site region in the ternary complex of activated MET with ATP and hexapeptide substrates. Backbone coloring and side-chains representation is the same as in Figure 2. **a:** Selected electrostatic (pink dashed lines) and hydrophobic (gray dots) interactions important for maintaining the active-site architecture. The position of mutation V1110I is marked by red sphere and the mutated Ile1110 side chain is shown in cyan. **b:** Conformation of the A-loop. The positions of mutations D1246N/H and Y1248H/D/C are marked by red spheres, and the mutated Asn1246 side chain is shown in cyan. Interactions stabilizing the active conformation of the A-loop after mutation D1246N are shown as cyan dashed lines; those maintained by nonphosphorylated tyrosines, as pink dashed lines.

Figure 3.

domain (Fig. 2) on the structures of the corresponding forms of IRK.[17,18]

Active Form of MET Kinase

The phosphorylated catalytic core domain of MET was modeled in complex with the MgATP molecule and a hexapeptide substrate comprising the sequence ATYVNV derived from the C-terminal self-phosphorylation site of MET. The RMS difference for the superposition of MET and IRK structures in their active forms is 0.9 Å for 248 Cα atom pairs. The orientation of the two lobes is the same as in the ternary complexes of other protein kinases. In these complexes, protein kinases were always found in the well-defined "closed" conformation.[16] The ATP molecule is bound at the interface of the two lobes [Fig. 2(a)] and is properly oriented for the phosphotransfer process by key interactions mainly with the side chains of residues conserved among kinases and via hydrogen bonds to the protein backbone. Positioning of the adenine ring between Val1110 from the N-terminal lobe and Met1229 from the C-terminal lobe defines the separation of the lobes in the active form. As in the IRK structure,[18] the β-phosphate group of ATP interacts with the backbone of the glycine-rich loop, whereas α- and β-phosphates contact Lys1128 [Fig. 3(a)]. The Mg^{2+} ions are coordinated by side-chain oxygens of Asp1240 from the kinase-conserved DFG motif and Asn1227 from the catalytic loop (data not shown). Residues from helix C play an important role in maintaining the active-site architecture. The conserved Glu1145 ensures the proper conformation of Lys1128 [Fig. 3(a)]; Ile1148 and Met1149 are part of the hydrophobic pocket for Phe1241 from the DFG triplet [Fig. 2(a) and data not shown].

None of the MET PRC mutations interfere with the active-site architecture. Ile instead of Val at position 1110 can be easily accommodated in the adenine-binding pocket [Fig. 3(a)] and will make van der Waals contacts with the aliphatic portion of the Lys1128 side chain, stabilizing its critical position during the catalytic process. The surface area of legitimate contacts between amino acid side chains at the position 1110 and Lys1128 increases twofold with the V1110I mutation. In the case of the M1149T mutation, only the interaction of Met1149 methyl group with Phe1241 will be lost, leaving the rest of the hydrophobic pocket for Phe1241 unchanged.

The A-loop is disengaged from the active site, allowing for binding of a peptide substrate [Fig. 3(b)]. Phosphorylated Tyr1248 (pTyr1248) is exposed to solvent, whereas pTyr1252 and pTyr1253 stabilize this conformation of the A-loop via an extensive network of interactions. The phosphate group of pTyr1252 makes ionic interactions with Lys1250, His1256, and Lys1277 from the C-terminal lobe of the enzyme. pTyr1253 was modeled as in the active form of IRK,[18] and it does not interact directly with Arg1221 (the kinase-conserved residue that immediately precedes catalytic Asp) but only with the guanidinium group of Arg1245. This is in contrast to the arrangement observed in the cAPK[43] and LcK[28] structures. Interactions of nonphosphorylated tyrosines from the A loop, Tyr1252 with Lys 1277 from the C-terminal lobe and Tyr1253 with

Arg1245, can be maintained via hydroxyl groups of the tyrosines. These observations suggest that triphosphorylation of the MET A loop is not critical for its enzymatic activity. Several MET PRC mutations contribute to stabilization of the active conformation of the A loop. Particularly important in this respect are the D1246N/H mutations. The side chain of Asn or His [Fig. 3(b)] in this position provides two additional hydrogen bonds, one to the main chain NH group of Tyr1248 from the A loop and the second to the main chain carbonyl of Lys1217 from β-strand 6, which precedes the catalytic loop. Both mutations provide an additional link between the A-loop and the C-terminal lobe, ensuring an active conformation. One has to bear in mind, however, that this conformation of the A-loop may be possible only with the peptide substrate bound in the active site. As shown by crystallographic and solution studies of the activating A-loop mutant of IRK, unphosphorylated A-loop disengaged from the active site is partially disordered and undergoes reconfiguration on peptide-substrate binding, before the catalytic step.[44]

MET PRC mutations located at the interfaces between the subdomains do not interfere with interactions maintaining the tertiary structure of the active form. Detailed analysis of van der Waals contacts (data not shown) revealed that the V1238I and V1206L mutations strengthen the packing of a hydrophobic cluster at the beginning of the flexible A-loop. In mutation L1213V, the substitution of Leu1213 by a smaller Val side chain will eliminate several hydrophobic interactions of Leu1213 with its surroundings, but it will simultaneously diminish the surface area of illegitimate contacts of Leu1213 with neighboring main-chain amide groups. Although the overall complementarity for either Leu or Val in this position is the same, that is, about 52 Å², due to loss of interactions between Cδ2 atoms from Leu1213 and Tyr1212, in the L1213V mutant MET, partially buried Tyr1212 will lose its anchor to the hydrophobic core of the molecule and most probably will adopt a solvent-exposed conformation.

Substrate Specificity

The hexapeptide substrate binds to the outer part of the active-site cleft and makes contacts with residues from the C-terminal lobe of the catalytic core. A short antiparallel β-sheet is formed between β-strand 11 from the A-loop and the three residues following Tyr P (the tyrosine to be phosphorylated) from the substrate: the backbone of Val P+1 and Val P+3 is hydrogen bonded to the backbone of Leu1263 and Ala1261, respectively. Interactions of the substrate's side chains with the enzyme residues (enzyme-binding pockets) are shown in Table I. Side chains P+1 and P+3 are located in well-defined hydrophobic pockets. The S+1 pocket includes side chains of Val1265, Thr1307, and Phe1308; the S+3 pocket comprises Leu1263, Val1265, and Met1268. The hydroxyl oxygen of Thr P-1 forms a hydrogen bond with the guanidinium group of Arg1226 from the catalytic loop, and the side chain amide of Asn P+2 with main-chain carbonyl of Gly1260. An additional hydrogen bond is formed between the main-chain atoms of Ala P-2 and the hydroxyl oxygen of Thr1307.

TABLE I. Interactions With Substrate Side Chains in Different Forms of MET[+]

Tail substrate	Ala P-2	Thr P-1	Val P+1	Asn P+2	Val P+3
Wild-type MET	Thr1307 (4.7) h	Arg1184 (3.1) e Arg1226 (23.9) e Arg1226 (4.3) h Trp1267 (2.2) h	Val1265 38.6) h Thr1307 (27.1) h Phe1308 (22.4) h	Gly1260m (22.8) e Lys1262 (1.7) h	Leu1263 (20.0) h Val1265 (19.5) h Met1268 (2.7) h
c-Abl substrate	**Gly P-2**	**Pro P-1**	**Ala P+1**	**Gln P+2**	**Pro P+3**
MET (M1268T)		Arg1226 (2.0) h Trp1267 (15.3) h	Val1265 (21.3) h Thr1307 (24.5) h Phe1308 (7.6) h	Gly1260m (15.2) e Lys1262 (9.9) h	Leu1263 (31.6) h Val1265 (7.2) h
A-loop	**Lys1250**	**Glu1251**	**Tyr1253**	**Ser1254**	**Val1255**
Wild-type MET (inhibited form)	Met1247m (21.4) e Pro1300 (4.7) h	Arg1184 (4.2) e Lys1266 (5.8) h Trp1267 (16.8) h	Val1265 (24.9) h Thr1307 (11.7) h Phe1308 (2.5) h	Lys1262 (4.9) e Lys1262 (4.9) h	Lys1258 (3.8) h Leu1263 (24.7) h Val1265 (24.9) h Leu1273 (10.1) h Thr1311 (11.9) h

[+]Surface area (Å^2) of legitimate contacts is given in parenthesis. e, electrostatic interactions; h, hydrophobic interactions; m, main chain atoms.

We studied the effect of the M1268T mutation on substrate specificity of the MET kinase by modeling and biochemical assays. This mutation changes the conserved sequence of the P+1 loop of RTKs into a sequence characteristic for cytosolic tyrosine kinases (Fig. 1). In view of the highly transforming properties of the phosphorylated form of CrkII,[37] a substrate for the cytosolic tyrosine kinase c-Abl, we investigated the level of CrkII phosphorylation by wild-type MET and three MET mutants: M1268T, Y1248H, and D1246H. As shown by Western analysis in Figure 4, Crk II was strongly phosphorylated in NIH 3T3 cells expressing the M1268T mutant MET, and to some extent in NIH 3T3 cells transfected with Y1248H and D1246H mutations, but not in cells expressing wild-type MET.

Modeling indicates that the modified P+1 loop of the M1268T mutant MET would interact well with the hexapeptide comprising the GPYAQP sequence derived from CrkII. Structural superposition of the C-terminal lobes of IRK and c-Src kinase showed that the backbone conformation of their P+1 loops is the same (data not shown). As shown in Figure 5, Thr at position 1268 can indeed be accommodated in the structure of MET without changes in the position of the main-chain atoms. The hydroxyl oxygen of the mutant Thr is hydrogen bonded to the main-chain carbonyl of Pro1264, whereas the methyl group forms hydrophobic contacts with Phe1278 and Leu1263. However, the proximity of Thr1268 Oγ1 restricts the conformation of the Val1265 side chain, which interacts with residues from the P+1 and P+3 subsites of the peptide substrate (Table I). The substitution of Met1268 by the smaller Thr enforces a conformational change of the Leu1263 side chain to maintain the proper packing in this area (Fig. 5 and Table II). As a result, the shape of the S+3 pocket is significantly changed. A detailed analysis of the interactions between bound hexapeptide and the P+1 loop in the constructed models is presented in Table III. To evaluate the influence of the M1268T mutation on substrate binding, we calculated the NC values for each complex. We found that the M1268T mutation slightly improves MET kinase interaction with its C-terminal tail phosphorylation site but may compromise substrate specificity (Table III). The difference in NC values between wild-type MET complexed with the hexapeptide from its C-terminal tail and from CrkII is 0.13, but the difference decreases to 0.09 in the case of M1268T mutant. This result is consistent with the experimental data shown in Figure 4 and with those reported by others.[13] Of the three mutationally activated (see below) MET proteins, only the M1268T mutant was able to phosphorylate the CrkII protein to a significant level (calculated NC value of 0.38). Even though Y1248H and D1246H mutations, as shown above, help to maintain the active conformation of MET kinase, their P+1 loops are not modified (corresponding NC value 0.33), and the levels of CrkII phosphorylation in cells expressing these mutants are lower. The difference in their efficiency may indicate the influence of residues located in the enzyme surface loop on binding of large protein substrates and/or the different level of kinase activation in these mutants.

Inhibited Form

In the unphosphorylated form of the wild-type MET, access to the ATP- and peptide-substrate-binding sites is blocked by the A-loop [Fig. 2(b)]. Phe1241 from the kinase-conserved triplet DFG occupies the adenine-binding pocket, and together with Gly1242, creates a steric hindrance, which holds apart the two lobes. Subdomain movement is also restricted by a small hydrophobic core (conserved in other PTKs) formed at the interference between the two lobes by the side chains of Phe1152, His1154, Val1157, Tyr1212, Leu1213, Phe1218, and the aliphatic portion of Lys1216. A segment comprising residues E^{1251}YYS^{1254} of the A-loop mimics peptide-substrate binding (Table I). Tyr1252 is hydrogen bonded to the catalytic aspartic acid, Asp1222, whereas the side chain of Tyr1253 is located in the S+1 binding pocket. The main chain of Val1255 diverges from the conformation adopted by the bound substrate, but its side-chain atoms form extensive interactions with the P+1 loop (Table I). The inhibitory conforma-

IP: anti Crk II
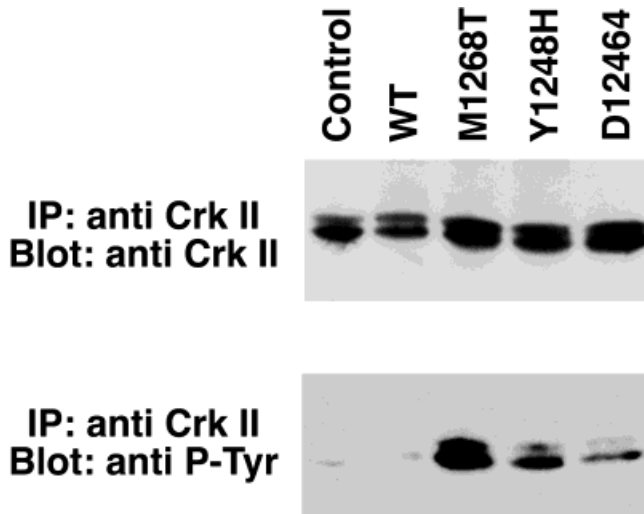Blot: anti Crk II

IP: anti Crk II
Blot: anti P-Tyr

Fig. 4. Phosphorylation of CrkII in wild-type and mutant MET-expressing cells after serum starvation. Samples labeled control and wild type are from cells stably transfected with the empty vector or vector expressing wild-type MET, respectively. All other samples are from cells stably transfected with vectors expressing the indicated mutant MET. Cells were cultured with DMEM/10% calf serum and serum starved for 16 h before harvest (top half of gel). Cell lysate (400 μg) was immunoprecipitated with CrkII antibody, resolved on an 8% polyacrylamide gel, and analyzed by Western blotting by using anti-Crk II antibody (bottom half of gel). The filter was then stripped and reprobed with antiphosphotyrosine antibody.

tion of the A-loop is further stabilized by hydrophobic interactions of the phenolic ring of Tyr1248 with aliphatic portions of Arg1226 and Arg1184 side chains and hydrogen bonds through its hydroxyl group to Asp1182 and Asn1185 (Fig. 6). Helix C is rotated relative to its position in the active form. Consequently, the interaction of Glu1145 with Lys1128 is lost. Carboxylate oxygens of Glu1145 form ionic interactions with the main-chain carbonyl of Gln1141 and the ring of His1106 from the glycine-rich loop (data not shown). Lys1128 is not properly oriented for coordination of ATP phosphates; instead, it is hydrogen bonded to the main-chain carbonyl of Phe1241 and contributes to the stabilization of the inhibitory conformation of the A-loop [Fig. 7(a)].

Mechanism of Ligand-Independent Activation of MET

Because of intrinsic flexibility of A-loop segments in RTKs, as revealed by high-temperature factors in the X-ray structures, most likely a spectrum of conformations with the unphosphorylated A-loop partially disengaged from the active site exists in vivo.[42] Solution studies of conformational flexibility in the A-loop of IRK showed that in the absence of ATP, 90% of the unphosphorylated IRK molecules exist in intrasterically inhibited state. However, in the presence of millimolar concentrations of Mg-adenine nucleotides, the equilibrium shifts toward more accessible conformations.[45] Monomeric RTKs exhibit weak basal enzymatic activity. The evidence suggests that substrates compete with the A-loop for binding in the active site cleft.[46] Ligand-induced receptor dimerization provides the peptide-substrate from one monomer properly positioned

for binding to the active site of the second monomer, thus activating the kinase. Subsequent transphosphorylation of tyrosines within the A-loop locks the enzyme in the activated form.

Transition to the active form requires a change in the relative position of the two lobes to permit productive ATP binding, access to the substrate-binding sites, and rotation of helix C to ensure proper placing of the DFG triplet and the coordination of ATP phosphate groups for the phospho-transfer reaction. Mutations may prompt the transition to the active form of the kinase by misplacing the A-loop from its inhibitory position and/or by facilitating subdomain movements. A shift of the equilibrium toward the active conformation can also be achieved by stabilizing the structure of MET kinase in its active form.

Mutations in the nucleotide-binding domain: V1110I, H1112Y/R, and H1124D

The replacement of Val1110 with Ile would result in a steric clash either with the ring of Phe1241 or with the side chain of Lys1128 [Fig. 7(a)]. Either one will force the A-loop out of the adenine-binding pocket, releasing the steric hindrance that prevents rearrangement of the two lobes.

His1112 and His1124 affect the position of Tyr1177, which closes the pocket for Phe1241 [Fig. 7(b)]. In the active form of MET, Tyr1177 (together with His1112 and His1124) is moved slightly away to accommodate the larger adenine ring. In the inactive form, positions of His1112 and His1124 are maintained by a network of hydrogen bonds: OCys1125—Nδ1His1112; Nε2His1112—Nδ1His1124; Nε2His1124—NζLys1179. Mutations H1112Y/R/L or H1124D will destroy these interactions and facilitate Tyr1177 movement.

Mutations in the hinge regions: M1149T, L1213V, V1206L, and V1238I

Because the conformational transition to the active state involves subdomain movements, this transition can be easily triggered by enhancement of flexibility in the tertiary structure at critical points. Met1149 plays an important role in imposing conformational constraints on the MET structure. Mutation M1149T will eliminate the hydrophobic interactions of Met1149 with the L1175 side chain and with the Phe1152 ring, which are critical for maintaining the spatial position of helix C in the inactive conformation of MET [Fig. 8(a)]. Loss of these constraints will promote helix C movement and, subsequently, the correct orientation of residues from the active site.

Ile substituting for Val at position 1238 clashes with one of the following residues: Ala1209, Met1210, Leu1213, Leu1223, and Cys1228. As a result, Ile1238, which precedes the first residue from the A-loop, is pushed out from the hydrophobic pocket formed by the side chains of Val1157, Val1206, Ala1209, Met1210, Leu1213, His1220, Leu1223, Cys1228, and Val1236 [Fig. 8(b)]. A similar effect is generated by the mutation of Val 1206 from this cluster to Leu, which results in steric clashes either with Cys1228 or Val1238. Substitution of Leu1213 by the smaller Val eliminates two van der Waals contacts:
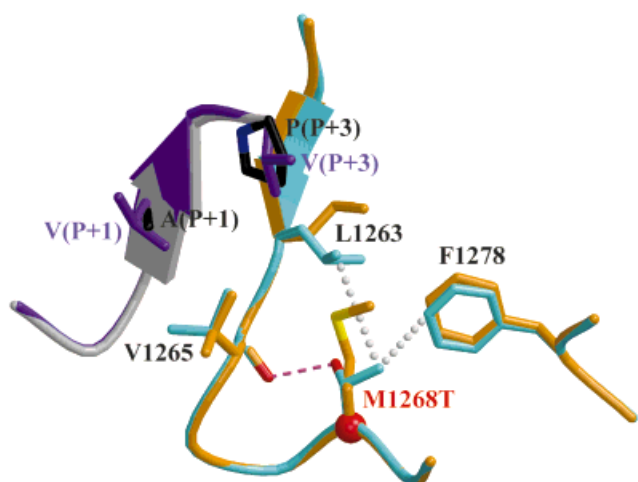
Fig. 5.   Comparison of substrate binding for wild-type and M1268T mutant MET. The P+1 loop is shown in orange and cyan and the bound peptide in violet and gray/black for wild-type and mutant MET complexes, respectively. The position of mutation M1268T is marked by a red sphere. Important hydrophobic interactions between the Thr 1268 side chain and neighboring residues in the MET mutant that maintain the proper internal packing are shown as pink dashed line and gray dots for hydrogen bond (see text) and hydrophobic contacts, respectively. Note the change in conformation of the Leu1263 side chain. The necessity of this change is documented in Table II.
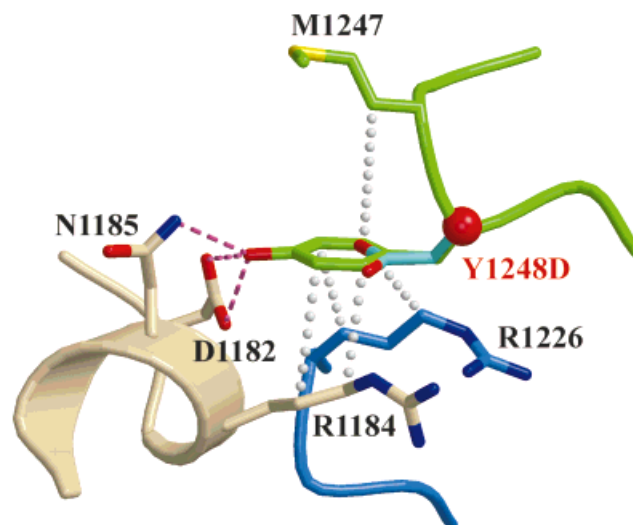

Fig. 6.   Interactions of the side chain of Tyr1248 from the A-loop with neighboring residues in the inhibited form of MET. Hydrogen bonds and hydrophobic contacts are represented by pink dashed lines and gray dots, respectively. The coloring of the backbone is the same as in Figure 2. The position of mutations Y1248H/D/C is marked by red sphere, and the mutated Asp 1248 side chain is shown in cyan.
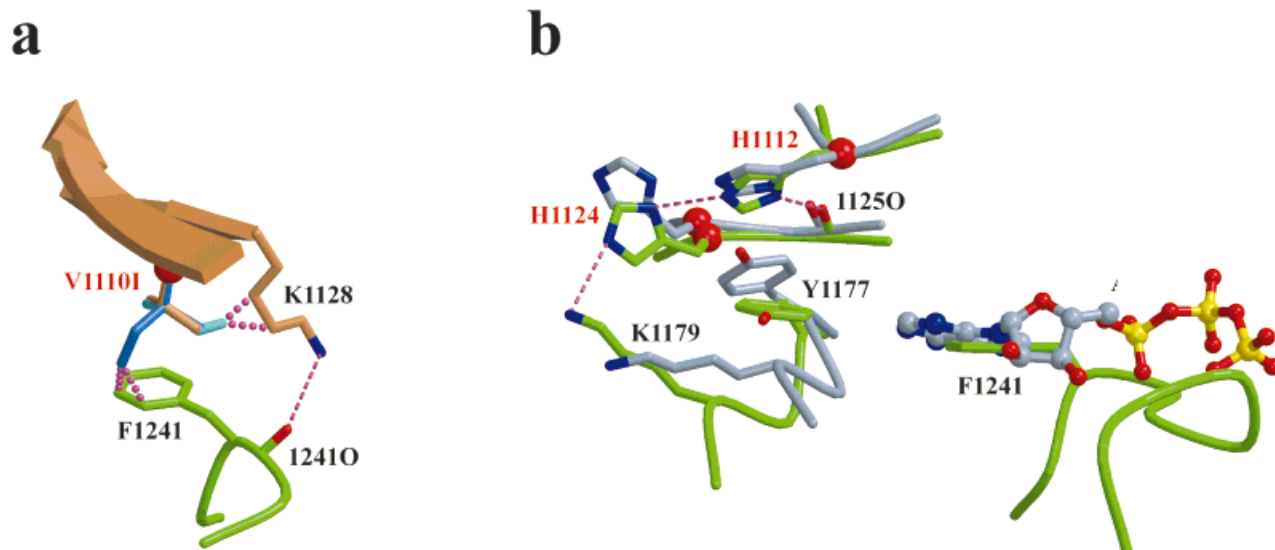

Fig. 7.   Activating mutations in the nucleotide-binding domain. **a:** Region of the V1110I mutation in the inhibited form of MET. The coloring of the backbone representation is the same as in Figure 2. The position of the V1110I mutation is marked by red sphere, and two selected side chain conformers of the mutated Ile 1110 are shown in cyan and light blue. The steric clashes between the atoms are represented by pink dots. **b:** Superposition of the N-terminal lobes of inhibited (green) and active (gray) forms of MET, showing important changes in the region of mutations at the 1112 and 1124 positions. Selected side chains are represented as sticks, and ATP is represented as balls and sticks. The positions of mutations H1112Y/R and H1124D are marked by red spheres. The network of hydrogen bonds exclusive for the inhibited form of MET is represented by pink dashed lines.

Leu1213 with Val1238, and Leu1213 with Phe1152 from the N-terminal lobe.

Mutations in the A-loop: D1246N/H and Y1248H/D/C

Replacing the buried Tyr1248 by the polar and shorter side chain of Asp or His eliminates the hydrophobic interactions of the phenolic ring with the aliphatic side chains of Arg1226 and Arg1184 as well as hydrogen bonds with the side chains of Asp1182 and Asn1185 (Fig. 6). In the case of the Y1248C mutation, both hydrogen bonds are also lost, and the number of hydrophobic contacts decreases dramatically (data not shown). These mutations will destabilize the inhibitory conformation of the A-loop. Similar to phosphorylated Tyr1248 these mutations

**TABLE II. Contact Surface Area Between Leu 1263 Side Chain and MET Core After Mutation M1268T
for Two Different Conformations of Leu 1263**

Enzyme	Conformation of Leu1263[a]	Contact surface area (Å^2)		
		Legitimate contacts	Illegitimate contacts	Complementarity
MET (M1268T) (active form)	1	77.8	−50.9	26.9
	2	96.9	−39.7	57.2
MET (M1268T) (inhibited form)	1	79.8	−51.4	28.4
	2	108.8	−35.9	72.9

[a]1, as in wt MET; 2, available after mutation M1268T.

**TABLE III. Comparison of Evaluated Affinities for MET and c-Abl Substrates in the Structures
of Wild-Type and Mutated MET Kinase**

Enzyme	Contact surface area (Å^2)			Normalized complementarity
	Legitimate contacts	Illegitimate contacts	Complementarity	
Wild-type MET + tail substrate	513.9	−81.0	432.9	0.46
MET (M1268T) + tail substrate	516.6	−76.5	440.1	0.47
Wild-type MET + c-Abl substrate	448.7	−120.4	328.3	0.33
MET (M1268T) + c-Abl substrate	455.8	−105.6	350.2	0.38

**TABLE IV. Legitimate Contacts Between Leu1263 Side Chain and Substrate Side Chains
in Different Forms of MET**

Enzyme	Substrate	Nearest distance (Å)	Contact surface (Å^2)
Wild-type MET (inhibited form)	Val1255	3.9	24.7
MET (M1268T) (inhibited form)	Val1255	4.1	12.4
Wild-type MET + tail site	ValP+3	4.1	10.5
MET (M1268T) + tail site	ValP+3	4.1	20.9
MET (M1268T) + c-Abl substrate	ProP+3	3.7	31.6

strongly favor the activated form, in which a residue at this position is fully exposed to solvent [Fig. 3(b)]. The D1246N mutation plays a role in stabilization of the active form (see above). In the inactive structure of IRK, the side chain of Asp1156 (equivalent to Asp1246 of MET) is disordered; thus this mutation is not expected to contribute to stabilization of the inactive conformation.

Mutation M1268T in the P+1 loop

Mutation M1268T leads to a change in the conformation of Leu1263. As indicated by the data in Table IV, this change has a profound effect on the interactions of Leu1263 with a substrate residue at the P+3 position. In the inhibited form of MET, this mutation diminishes interactions of the P+1 loop with the part of the A-loop that mimics bound substrate (i.e., the contact surface area between the Leu1263 side chain and Val1255 decreases twofold), destabilizing the inhibitory position of the loop. Conversely, in the active form, the M1268T mutation increases the contact surface area of Leu1263 with Val P+3 twofold, and threefold with Pro P+3 from the c-Abl substrate, CrkII. This finding presents a possibility that some substrates (e.g., CrkII and MET C-terminal domain) may successfully compete with the A-loop for the substrate-binding site of the M1268T MET mutant and undergo

phosphorylation in the absence of the A-loop phosphorylation. Because a Val residue occupies the P+3 position in respect to both tyrosine residues from the Met C-terminal autophosphorylation site, the C-terminal tail can be phosphorylated by the M1268T mutant in this manner on both tyrosine residues. This is not the case for the wild-type MET (see reversed values of contact surface area for Val1255 and Val P+3 with Leu1263 in the active and inactive forms), which first must be activated by transphosphorylation of the A-loop. Extensive phosphorylation of a peptide containing the MET docking site by the M1268T mutant, but not by the wild-type MET, was shown in vitro.[13] In addition, the full-size M1268T MET mutant was found phosphorylated and constitutively bound to c-Src in the absence of HGF.[47] Taken together, these data indicate that the effect on kinase activation by this mutation will depend on the substrate.

Summary

The analysis presented here allows an understanding at the molecular level of the mechanism of MET kinase activation in the absence of the specific ligand. We showed that MET PRC mutations interfere with the intrasteric mechanism of tyrosine kinase autoinhibition and facilitate transition to the active form of the enzyme. MET PRC
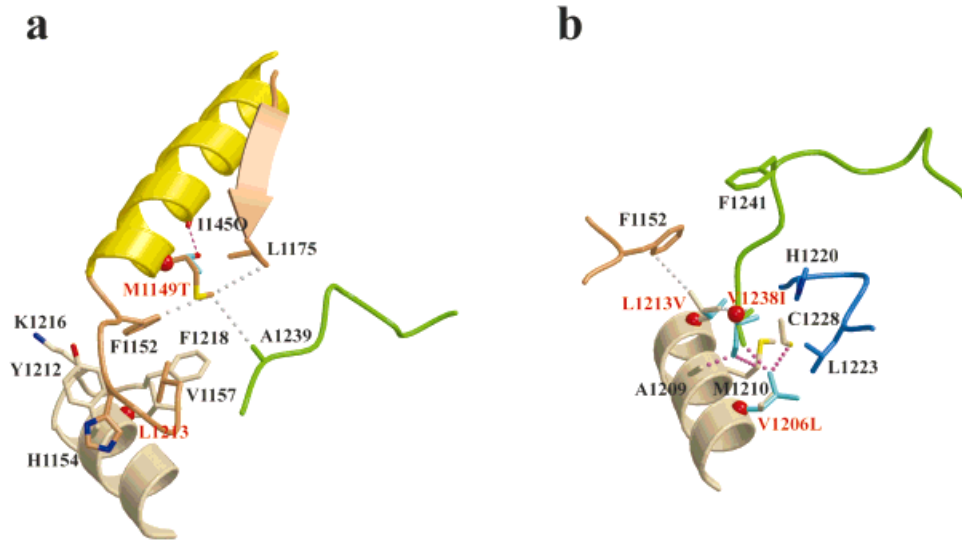
Fig. 8. Enlargement of the hinge region in the inhibited form of MET, showing the effects of mutations (**a**) M1149T and (**b**) V1206L, L1213V, and V1238I. The coloring of the backbone is the same as in Figure 2. The positions of the activating mutations are marked by red spheres, and the mutated side chains are shown in cyan. The hydrogen bonds are represented by pink dashed lines, and hydrophobic contacts and steric clashes by gray and pink dots, respectively.
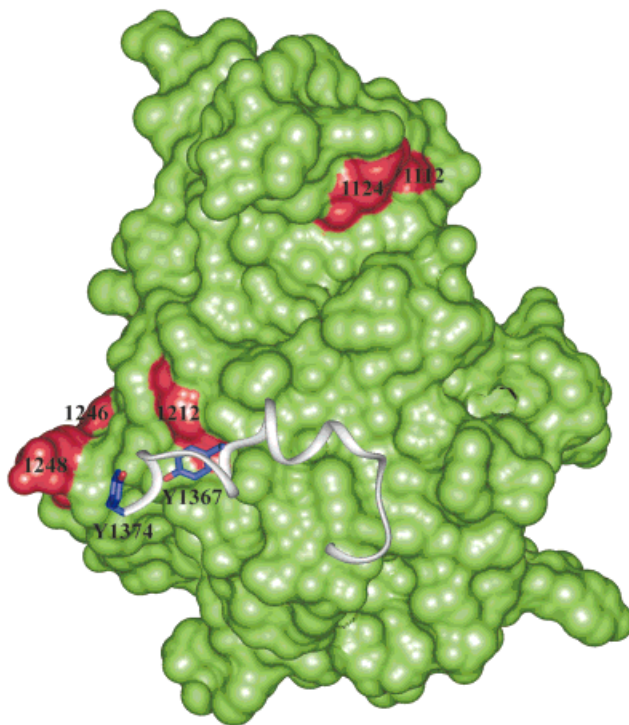

Fig. 9. The molecular surface of the active form of MET kinase domain. Contributing area from His1112, His1124, Tyr1212, Asp1246, and Tyr1248 is shown in red. View is rotated from that in Figure 2(a). Segment of C-terminal tail comprising MET residues 1356–1374 (modeled as the corresponding region in the IRKP3 structure) is shown as white ribbon; docking site tyrosine residues are colored violet.

mutations increase the level of basal kinase activity of the MET receptor with different efficiency. In the presence of physiological concentrations of ATP, the A-loop of IRK is partially disengaged from the active site in a large fraction of the unphosphorylated receptor population.[45] Thus, activating potential of MET mutations located in the nucleotide-binding domain is very low,[11] whereas mutations in the A-loop, which stabilize its outward conformation, exhibit a high level of constitutive kinase activation.[12] Results reported in this study indicate that the M1268T mutation in the P+1 loop is the only one PRC mutation that weakens the interactions between the A-loop and the peptide-substrate-binding site of MET protein. The M1268T MET mutant has altered substrate specificity, and its enzymatic activity is driven by the competition between the peptide-substrate and the A-loop for binding to the catalytic site.

BIOLOGICAL IMPLICATIONS

The biological effect of PRC mutations varies among mutants, and their activities depend to different extents on the presence of HGF and the level of MET expression. Addition of the specific ligand for MET not only further activates the kinase but also brings to the proximity of its active site the C-terminal phosphorylation site, which mediates most MET signaling pathways. The M1268T MET mutant is the least sensitive to the stimulation by HGF.[15] Our results suggest that this mutant can phosphorylate the C-terminal tail of MET and substrates specific for cytosolic tyrosine kinases such as CrkII without ligand-mediated activation of MET kinase. Therefore, the effect of the M1268T mutant MET will depend mainly on the concentration of its possible substrates (e.g., on the level of MET expression and cellular content). Substitution of Tyr1248 by a polar residue, which cannot be accommodated in the inhibited form, makes the activated kinase "immune" to the action of phosphatases, thus further deregulating enzymatic activity. A deregulated wild-type kinase activity can adequately explain oncogenic potential in the case of germline mutations. The hereditary form of

PRC has been found only in adults[10,11]; therefore, any mutational change in pathways critical for embryonic development is unlikely. Neoplastic transformation develops slowly, probably by the same mechanism as in cells that coexpress the unmodified MET and HGF.[6] Somatic mutations, as well as the germline mutation Y1248C, alter pathways invoked by wild-type MET[13,14] in addition to increasing enzymatic activity. For the most adverse somatic mutation, M1268T, the change in substrate specificity may be responsible for the mutant's transforming properties in vitro and tumorigenicity in vivo. In view of the recent results on the essential role of GAB1 for signaling by the MET receptor,[48,49] an aberrant phosphorylation of the GAB1 adaptor by the M1268T mutant is a possibility. All other somatic mutations, except L1213V, are located on the surface of the MET kinase domain (Fig. 9). Although Leu1213 is buried, the L1213V mutation may prompt Tyr1212 to adopt a conformation fully exposed to environment (above). Tyr1212 seems to play an important role in signaling *via* oncogenic forms of MET[50] by a mechanism that is yet not determined. A hypothesis that Tyr1212 is a site of phosphorylation was put forward but could not be confirmed.[50]

Activation of the complex network of MET-mediated signal transduction pathways requires a long sequence of molecular events. A change in the molecular surface, particularly if it occurs in a location critical for signaling, can disturb the interdomain and/or intermolecular interactions of MET, affecting cellular responses mediated by the wild-type protein. Codons 1212, 1246, and 1248 are situated in close proximity to each other [Fig. 2(a) and Fig. 9]. Analogy with the activated IRK structure may offer a possible explanation for the role in oncogenesis played by residues occupying these positions. If the C-terminal tail (extending beyond the kinase-conserved catalytic domain) of MET follows a path similar to the one observed for IRK,[18] Tyr1367 and Tyr1374 from the MET docking site would be situated in the vicinity of cytosol-exposed residues 1246 and 1248 from the A-loop, as well as Tyr1212 at the end of helix E (Fig. 9). MET mutations in PRC at codons 1246, 1248, and 1213 may alter fidelity of the C-terminus phosphorylation and/or directly interfere with the binding of certain effector molecules. Thus, signaling via MET activated by different point mutations can exert distinct and unique biological consequences.

ACKNOWLEDGMENTS

REFERENCES

1. Ponzetto C, Bardelli A, Zhen Z, Maina F, dalla ZP, Giordano S, Graziani A, Panayotou G, Comoglio PM. A multifunctional docking site mediates signaling and transformation by the hepatocyte growth factor/scatter factor receptor family. Cell 1994;77:261–271.

2. Weidner KM, Sachs M, Riethmacher D, Birchmeier W. Mutation of juxtamembrane tyrosine residue 1001 suppresses loss-of-function mutations of the met receptor in epithelial cells. Proc Natl Acad Sci USA 1995;92:2597–2601.

3. Tulasne D, Paumelle R, Weidner KM, Vandenbunder B, Fafeur V. The multisubstrate docking site of the MET receptor is dispensable for MET-mediated RAS signaling and cell scattering. Mol Biol Cell 1999;10:551–565.

4. Weidner KM, Di Cesare S, Sachs M, Brinkmann V, Behrens J, Birchmeier W. Interaction between Gab1 and the c-Met receptor tyrosine kinase is responsible for epithelial morphogenesis. Nature 1996;384:173–176.

5. Uehara Y, Minowa O, Mori C, Shiota K, Kuno J, Noda T, Kitamura N. Placental defect and embryonic lethality in mice lacking hepatocyte growth factor/scatter factor. Nature 1995;373:702–705.

6. Jeffers M, Rong S, Woude GF. Hepatocyte growth factor/scatter factor-Met signaling in tumorigenicity and invasion/metastasis. J Mol Med 1996;74:505–513.

7. Santoro M, Carlomagno F, Romano A, Bottaro DP, Dathan NA, Grieco M, Fusco A, Vecchio G, Matoskova B, Kraus MH. Activation of RET as a dominant transforming gene by germline mutations of MEN2A and MEN2B. Science 1995;267:381–383.

8. Smith DP, Houghton C, Ponder BA. Germline mutation of RET codon 883 in two cases of de novo MEN 2B. Oncogene 1997;15:1213–1217.

9. Pignon JM. C-kit mutations and mast cell disorders: a model of activating mutations of growth factor receptors. Hematol Cell Ther 1997;39:114–116.

10. Schmidt L, Duh FM, Chen F, Kishida T, Glenn G, Choyke P, Scherer SW, Zhuang Z, Lubensky I, Dean M, Allikmets R, Chidambaram A, Bergerheim UR, Feltis JT, Casadevall C, Zamarron A, Bernues M, Richard S, Lips CJ, Walther MM, Tsui LC, Geil L, Orcutt ML, Stackhouse T, Lipan J, Slife L, Brauch H, Decker J, Niehans G, Hughson MD, Moch H, Storkel S, Lerman MI, Linehan WM, Zbar B. Germline and somatic mutations in the tyrosine kinase domain of the MET proto-oncogene in papillary renal carcinomas. Nat Genet 1997;16:68–73.

11. Schmidt L, Junker K, Nakaigawa N, Kinjerski T, Weirich G, Miller M, Lubensky I, Neumann HP, Brauch H, Decker J, Vocke C, Brown JA, Jenkins R, Richard S, Bergerheim U, Gerrard B, Dean M, Linehan WM, Zbar B. Novel mutations of the MET proto-oncogene in papillary renal carcinomas. Oncogene 1999;18:2343–2350.

12. Jeffers M, Schmidt L, Nakaigawa N, Webb CP, Weirich G, Kishida T, Zbar B, Vande Woude GF. Activating mutations for the met tyrosine kinase receptor in human cancer. Proc Natl Acad Sci USA 1997;94:11445–11450.

13. Bardelli A, Longati P, Gramaglia D, Basilico C, Tamagnone L, Giordano S, Ballinari D, Michieli P, Comoglio PM. Uncoupling signal transducers from oncogenic MET mutants abrogates cell transformation and inhibits invasive growth. Proc Natl Acad Sci USA 1998;95:14379–14383.

14. Giordano S, Maffe A, Williams TA, Artigiani S, Gual P, Bardelli A, Basilico C, Michieli P, Comoglio PM. Different point mutations in the met oncogene elicit distinct biological properties. FASEB J 2000;14:399–406.

15. Michieli P, Basilico C, Pennacchietti S, Maffe A, Tamagnone L, Giordano S, Bardelli A, Comoglio PM. Mutant Met-mediated transformation is ligand-dependent and can be inhibited by HGF antagonists. Oncogene 1999;18:5221–5231.

16. Cox S, Radzio-Andzelm E, Taylor SS. Domain movements in protein kinases. Curr Opin Struct Biol 1994;4:893–901.

17. Hubbard SR, Wei L, Ellis L, Hendrickson WA. Crystal structure of the tyrosine kinase domain of the human insulin receptor. Nature 1994;372:746–754.

18. Hubbard SR. Crystal structure of the activated insulin receptor tyrosine kinase in complex with peptide substrate and ATP analog. EMBO J 1997;16:5572–5581.

19. Mohammadi M, Schlessinger J, Hubbard SR. Structure of the

FGF receptor tyrosine kinase domain reveals a novel autoinhibitory mechanism. Cell 1996;86:577–587.

20. Mohammadi M, McMahon G, Sun L, Tang C, Hirth P, Yeh BK, Hubbard SR, Schlessinger J. Structures of the tyrosine kinase domain of fibroblast growth factor receptor in complex with inhibitors. Science 1997;276:955–960.

21. Mohammadi M, Froum S, Hamby JM, Schroeder MC, Panek RL, Lu GH, Eliseenkova AV, Green D, Schlessinger J, Hubbard SR. Crystal structure of an angiogenesis inhibitor bound to the FGF receptor tyrosine kinase domain. EMBO J 1998;17:5896–5904.

22. Martin AC, MacArthur MW, Thornton JM. Assessment of comparative modeling in CASP2. Proteins 1997;Suppl 1:14–28.

23. Xu W, Harrison SC, Eck MJ. Three-dimensional structure of the tyrosine kinase c-Src. Nature 1997;385:595–602.

24. Williams JC, Weijland A, Gonfloni S, Thompson A, Courtneidge SA, Superti-Furga G, Wierenga RK. The 2.35 A crystal structure of the inactivated form of chicken Src: a dynamic molecule with multiple regulatory interactions. J Mol Biol 1997;274:757–775.

25. Xu W, Doshi A, Lei M, Eck MJ, Harrison SC. Crystal structures of c-Src reveal features of its autoinhibitory mechanism. Mol Cell 1999;3:629–638.

26. Sicheri F, Moarefi I, Kuriyan J. Crystal structure of the Src family tyrosine kinase Hck. Nature 1997;385:602–609.

27. Schindler T, Sicheri F, Pico A, Gazit A, Levitzki A, Kuriyan J. Crystal structure of Hck in complex with a Src family-selective tyrosine kinase inhibitor. Mol Cell 1999;3:639–648.

28. Yamaguchi H, Hendrickson WA. Structural basis for activation of human lymphocyte kinase Lck upon tyrosine phosphorylation. Nature 1996;384:484–489.

29. Homology User Guide, Version 95.0. San Diego: Biosym Technologies; 1995.

30. Thompson JD, Higgins DG, Gibson TJ. CLUSTAL W: improving the sensitivity of progressive multiple sequence alignment through sequencing weighting, position-specific gap penalties and weight matrix choice. Nucleic Acids Res 1994;22:4673–4680.

31. Discover User Guide, Version 95.0. San Diego: Biosym Technologies; 1995.

32. Weiner SJ, Kollman PA, Case DA, Singh UC, Ghio C, Alagona G, Profeta SJr, Weiner P. A new forcefield for molecular mechanical simulation of nucleic acids and proteins. J Am Chem Soc 1984;106: 765–784.

33. Becke AD. Density-functional thermochemistry. III. The role of exact exchange. J Chem Phys 1993;5648–5652.

34. Frisch MJ, Trucks GW, Schlegel HB, Gill PMW, Johnson BG, Robb MA, Cheeseman JR, Keith T, Petersson GA, Montgomery JA, Raghavachari K, Al-Laham MA, Zakrzewski VG, Oritz JV, Foresman B, Cioslowski J, Stefanov BB, Nanayakkara A, Challacombe M, Peng CY, Ayala PY, Chen W, Wong MW, Andres JL, Replogle ES, Gomperts R, Martin RL, Fox DJ, Binkley JS, Defrees DJ, Baker J, Steward JP, Head-Gordon M, Gonzalez C, Pople JA. Gaussian 94. Pittsburgh, PA: Gaussian, Inc.; 1995.

35. Hooft RW, Vriend G, Sander C, Abola EE. Errors in protein structures [letter]. Nature 1996;381:272.

36. Bower MJ, Cohen FE, Dunbrack RL Jr. Prediction of protein side-chain rotamers from a backbone-dependent rotamer library: a new homology modeling tool. J Mol Biol 1997;267:1268–1282.

37. Feller SM, Knudsen B, Hanafusa H. c-Abl kinase regulates the protein binding activity of c-Crk. EMBO J 1994;13:2341–2351.

38. Sobolev V, Sorokine A, Prilusky J, Abola EE, Edelman M. Automated analysis of interatomic contacts in proteins. Bioinformatics 1999;15:327–332.

39. Sobolev V, Wade RC, Vriend G, Edelman M. Molecular docking using surface complementarity. Proteins 1996;25:120–129.

40. Sobolev V, Moallem TM, Wade RC, Vriend G, Edelman M. CASP2 molecular docking predictions with the LIGIN software. Proteins 1997;Suppl 1:210–214.

41. Jeffers M, Fiscella M, Webb CP, Anver M, Koochekpour S, Vande Woude GF. The mutationally activated Met receptor mediates motility and metastasis. Proc Natl Acad Sci USA 1998;95:14417–14422.

42. Hubbard SR, Mohammadi M, Schlessinger J. Autoregulatory mechanisms in protein-tyrosine kinases. J Biol Chem 1998;273: 11987–11990.

43. Knighton DR, Zheng JH, Ten Eyck LF, Ashford VA, Xuong NH, Taylor SS, Sowadski JM. Crystal structure of the catalytic subunit of cyclic adenosine monophosphate-dependent protein kinase. Science 1991;253:407–414.

44. Till JH, Ablooglu AJ, Frankel M, Bishop SM, Kohanski RA, Hubbard SR. Crystallographic and solution studies of an activation loop mutant of the insulin receptor tyrosine kinase: insights into kinase mechanism. J Biol Chem 2001;276:10049–10055.

45. Frankel M, Bishop SM, Ablooglu AJ, Han YP, Kohanski RA. Conformational changes in the activation loop of the insulin receptor's kinase domain. Protein Sci 1999;8:2158–2165.

46. Weiss A, Schlessinger J. Switching signals on or off by receptor dimerization. Cell 1998;94:277–280.

47. Nakaigawa N, Weirich G, Schmidt L, Zbar B. Tumorigenesis mediated by MET mutant M1268T is inhibited by dominant-negative Src. Oncogene 2000;19:2996–3002.

48. Sachs M, Brohmann H, Zechner D, Muller T, Hulsken J, Walther I, Schaeper U, Birchmeier C, Birchmeier W. Essential role of Gab1 for signaling by the c-Met receptor in vivo. J Cell Biol 2000;150: 1375–1384.

49. Schaeper U, Gehring NH, Fuchs KP, Sachs M, Kempkes B, Birchmeier W. Coupling of Gab1 to c-Met, Grb2, and Shp2 mediates biological responses. J Cell Biol 2000;149:1419–1432.

50. Jeffers M, Koochekpour S, Fiscella M, Sathyanarayana BK, Vande Woude GF. Signaling requirements for oncogenic forms of the Met tyrosine kinase receptor. Oncogene 1998;17:2691–2700.

51. Kabsch W, Sander C. Dictionary of protein secondary structure: pattern recognition of hydrogen-bonded and geometrical features. Biopolymers 1983;22:2577–2637.